Monte-Carlo Simulation of Cooperative Localization Techniques for Inter-Vehicle Distance Estimation

Morteza Alijani[1,*,†], Andrea Steccanella[2], Wout Joseph[1,†], David Plets[1,†] and Daniele Fontanelli[3]

[1]*Department of Information Technology, imec-WAVES/Ghent University, Technologiepark-Zwijnaarde 126, 9052 Ghent, Belgium*

[2]*Centro Ricerche Fiat (CRF), SWX-Technologies & Components, Via Sommarive, 18 - 38123 Povo, Trento, Italy*

[3]*Department of Industrial Engineering, University of Trento, Via Sommarive, 9 - 38123 Povo, Italy*

Abstract

This paper presents a simulation study of non-ranging-based cooperative positioning algorithms, including absolute position differencing (APD), single-differencing (SD), single-differencing with a single satellite (SD-SS), and double-differencing (DD), for estimating the Inter-Vehicle Distance (IVD) of two static autonomous vehicles. To this end, a simplified scenario with two autonomous vehicles separated by 5.2 meters and receiving 99 epochs of Global Navigation Satellite System (GNSS) observables (also called the pseudorange) from four GPS satellites are considered. Then, a Monte-Carlo simulation is performed to investigate the performance of the APD, SD, SD-SS, and DD algorithms with different levels of pseudorange uncertainties, which are assumed to be uncorrelated and have zero means (i.e., no bias). The simulation results demonstrated that there is no significant difference between SD-based and DD-based approaches when four satellites are employed. Indeed, the systematic effects affecting the pseudorange measurements appear to be cancelled out. This is somehow expected since every satellite system suffers from different systematic measurement uncertainties. The results also indicate that the DD-based technique has a lower average IVD estimation error than the SD-SS algorithm since it can eliminate pseudorange uncertainties and any other common biases, implying that using the DD-based algorithm with multiple satellite systems may result in higher accuracy in the IVD estimation problem.

Keywords

Inter-Vehicle Distance (IVD), Monte-Carlo Simulation, Absolute Position Differencing (APD), Single-Differencing (SD), Double-Differencing (DD), Multiple Satellites

1. Introduction

Autonomous vehicles (AVs) represent a potentially disruptive change for different sectors ranging from industries to transportation. For example, AVs have the potential to improve future mobility by reducing traffic congestion, increasing vehicle safety, and boosting the energy efficiency of transportation systems [1]. At the heart of AV, the advanced driver-assistance system (ADAS) heavily depends on vehicle location and Inter-Vehicle Distance (IVD) measurements [2].

Proceedings of the Work-in-Progress Papers at the 13th International Conference on Indoor Positioning and Indoor Navigation (IPIN-WiP 2023), September 25–28, 2023, Nuremberg, Germany

*Corresponding author.

†These authors have the same affiliation.

morteza.alijani@ugent.be (M. Alijani); andrea.steccanella@crf.it (A. Steccanella); wout.joseph@ugent.be (W. Joseph); david.plets@ugent.be (D. Plets); daniele.fontanelli@unitn.it (D. Fontanelli)

© 2023 Copyright for this paper by its authors. Use permitted under Creative Commons License Attribution 4.0 International (CC BY 4.0).

CEUR Workshop Proceedings (CEUR-WS.org)

It is possible to use sensor-based (on-vehicle sensors) technologies such as radio detection and ranging (Radar), light detection and ranging (LiDAR)[3], or employing a camera system [4] to obtain a more accurate autonomous vehicle position and the vehicle relative distance to its surrounding objects or other vehicles. However, they are faced with constraints such as high cost and insufficient efficiency in harsh weather conditions, as well as limited perceptual fields [5]. To address the issues of sensor-based technologies, cooperative positioning algorithms, either ranging-based or non-ranging-based, can be employed [6]. For IVD estimation in ranging-based methods, signal strength variations such as radio signal strength [7], Time of Arrival [8], round trip time [9] or Time Difference of Arrival [10] can be used. However, these approaches are often costly since they require additional infrastructure and hardware to be implemented. In addition, the fast vehicle speed may also introduce noise or errors in estimated distances [6]. The non-ranging cooperative localization algorithm that directly utilizes each vehicle's pseudorange measurements can be used as a cost-effective alternative for vehicle localization and IVD estimation thanks to Global Navigation Satellite System (GNSS) observables [11],[12]. Notice that a pseudorange is an estimation of the distance between the antennas of the satellite orbiting the Earth and the GNSS receiver installed on the vehicle on the ground [11].

Several research studies have extended the concept of non-ranging cooperative positioning algorithms for IVD estimation [6],[11–13]. Tahir et al.[12] proposed four non-ranging-based IVD estimation methods as Absolute Position Differencing (APD), Pseudorange Differencing (PD), Single Differencing (SD), and Double Differencing (DD). While previous studies [6],[12] have broadly examined the IVD estimation problem using GNSS measurements, these studies have been limited to only one satellite (i.e., Galileo) and have not taken into account the Multi-Constellation Multi-Frequency (MCMF) system. MCMF systems are now widely available and have the potential to achieve centimeter-level accuracy [13,14], hence boosting the overall robustness of the system. For example, a study [13] investigating IVD estimation using multi-GNSS in a real-world application reported an absolute IVD estimation error of 42.24 cm and 12.20 cm when two and four satellite systems are employed, respectively.

The purpose of this study is to investigate the basis of four non-ranging-based cooperative positioning algorithms for IVD estimation, including APD, SD, single-differencing with a single satellite (SD-SS), and DD, as well as the impact of using multi-GNSS systems on the mentioned algorithms performance when using single and multiple satellite systems. It should be emphasized that this simulation and modelling are preliminary steps before evaluating the performance of the four aforementioned approaches when employing real pseudorange measurements. We describe the mathematical modelling of the pseudorange measurements and the formulation of non-ranging-based cooperative positioning algorithms in Section 2. Section 3 provides the Monte-Carlo simulation setup. Section 4 discusses the obtained simulated results, and finally, conclusions and future works are provided in Section 5.

2. Mathematical Modelling and Formulation

2.1. GNSS pseudorange model

The GNSS observables (raw code pseudorange) denoted by ρ, are defined as the estimated distance between the GNSS receiver installed on vehicle $V \in \{V_1, V_2, V_3, .., V_n\}$ and a satellite

$S \in \{S_1, S_2, S_3, .., S_A\}$ at any time-step k, which are modeled as follows [6],[12]:

$$\rho_V^S(k) = R_V^S(k) + t_V^S(k) + \varepsilon_c^S(k) + \varepsilon_u^S(k) \tag{1}$$

where $R_V^S(k) = \|\overrightarrow{P_S}(k) - \overrightarrow{P_V}(k)\|$ is the true geometric range between vehicle V and satellite S, the symbol $\|.\|$ represents the l_2 norm operation, $\overrightarrow{P_S}(k) = [x_S(k), y_S(k), z_S(k)]^T$ is the position vector of satellite S, $\overrightarrow{P_V}(k) = [x_V(k), y_V(k), z_V(k)]^T$ is the true position vector of vehicle V on the Earth-centered, Earth-fixed (ECEF) coordinate system, $t_V^S(k)$ is the clock misalignment error between the GNSS receiver installed on the vehicle V and satellite S, $\varepsilon_c^S(k)$ indicates the correlated (common) uncertainty induced by the ephemeris and the atmosphere, and finally, $\varepsilon_u^S(k)$ denotes the uncorrelated uncertainty, which includes the multi-path error, the thermal noise, and other residual errors [12].

It is considered that the correlated errors for various satellites are equivalent if the localized vehicles are close [6],[12]. Furthermore, obtaining a model for the uncorrelated errors is extremely challenging due to the presence of multipath. If the receiver is static, however, the first-order Auto-Regressive (AR) model is an excellent choice, which is given by [15]:

$$\varepsilon_u^S(k) = C\varepsilon_u^S(k-1) + n_u(k) \tag{2}$$

where C indicates the dimensionless AR coefficient value between 0 and 1, $n_u(k)$ represents a normally distributed random variable and follows the Gaussian distribution with zero mean and variance σ_u^2 i.e., $n_u(k) \sim (0, \sigma_u^2)$ [6],[12].

2.2. Cooperative Positioning Algorithms

2.2.1. Absolute Position Differencing (APD)

The GNSS receiver installed on each vehicle is able to compute an estimate of its absolute position vector in ECEF coordinates after acquiring and tracking the GNSS signal of at least four satellites. The absolute position differencing (APD) method calculates the estimated distance between two vehicles at any time-step k denoted by $\hat{D}_{ij}(k) = ||\overrightarrow{P_{V_j}}(k) - \overrightarrow{P_{V_i}}(k)||$, i.e.

$$\hat{D}_{ij}(k) = \sqrt{(z_{V_j} - z_{V_i})^2 + (y_{V_j} - y_{V_i})^2 + (x_{V_j} - x_{V_i})^2} \tag{3}$$

where $\overrightarrow{P_{V_i}}(k) = [x_{V_i}(k), y_{V_i}(k), z_{V_i}(k)]^T$ and $\overrightarrow{P_{V_j}}(k) = [x_{V_j}(k), y_{V_j}(k), z_{V_j}(k)]^T$ are the estimated position vectors of vehicle i and vehicle j obtained at time-step k from the GNSS in ECEF coordinates, respectively.

2.2.2. Single-Differencing (SD-based) algorithm

Fig.1 depicts the single differencing used for the IVD. The SD method estimates the IVD by subtracting the pseudorange measurements of two vehicles from the same satellite. This approach can eliminate both the clock imperfect synchronization between the vehicles as well as the atmospheric delay error. Given that the satellite S is sufficiently far from vehicles, the pseudorange measurements from each vehicle toward the satellite S are considered to be parallel

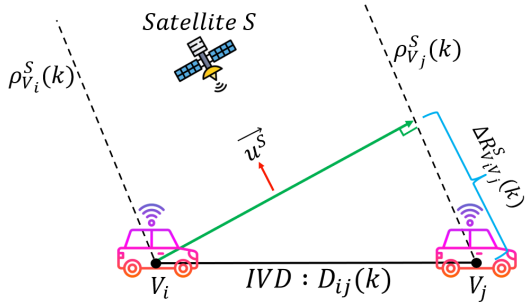

Figure 1: Single-Differencing (SD-based) IVD estimation algorithm

(see Fig.1) [6],[12]. More precisely, given (1) for two vehicles V_i and V_j, when computing the difference we have:

$$\Delta\rho^S_{V_iV_j}(k) = \rho^S_{V_i}(k) - \rho^S_{V_j}(k) = \Delta R^S_{V_iV_j}(k) + \Delta t_{V_iV_j}(k) + \Delta\varepsilon_{u_0}(k) \tag{4}$$

where $\Delta R^S_{V_iV_j}(k) = R^S_{V_i}(k) - R^S_{V_j}(k)$ defines the difference between the true distance of vehicle V_i and vehicle V_j from the satellite S, $\Delta t_{V_iV_j}(k) = t^S_{V_i}(k) - t^S_{V_j}(k)$ denotes the time delay error, and $\Delta\varepsilon_{u_0}(k) = \varepsilon^S_{u_{V_i}}(k) - \varepsilon^S_{u_{V_j}}(k)$ represents all the remaining uncertainties, usually dubbed *unusual error* [6],[12]. Due to the difference among the measured pseudoranges, the unusual error appears to be increasing [6]. Since the true distances between the vehicles and the satellites ($R^S_{V_i}(k)$ and $R^S_{V_j}(k)$), are much larger than the distance between the vehicles, we can estimate the $\Delta R^S_{V_iV_j}(k)$ as follows [6],[12]:

$$\Delta R^S_{V_iV_j}(k) = [\overrightarrow{u}^S]^T \overrightarrow{D_{ij}}(k) \tag{5}$$

where $\overrightarrow{u}^S = \frac{\overrightarrow{P_S}(k) - \overrightarrow{P_{V_i}}(k)}{\|\overrightarrow{P_S}(k) - \overrightarrow{P_{V_i}}(k)\|}$ is the Line-Of-Sight (LOS) unit vector from vehicle V_i to satellite S, $\overrightarrow{D_{ij}}(k)$ indicates the vehicle distance vector, $\overrightarrow{P_S}(k)$ represents the position vector of the satellite S and $\overrightarrow{P_{V_i}}(k)$ defines the position vector of the reference vehicle V_i at time-step k (see Fig.1 for reference). By considering N common visible satellites for the two vehicles and using (4), we can build the following measurement matrix:

$$\begin{bmatrix} \Delta\rho^1_{V_iV_j}(k) \\ \Delta\rho^2_{V_iV_j}(k) \\ \vdots \\ \Delta\rho^N_{V_iV_j}(k) \end{bmatrix} \approx \begin{bmatrix} [u^1]^T & 1 \\ [u^2]^T & 1 \\ \vdots & \vdots \\ [u^N]^T & 1 \end{bmatrix} \begin{bmatrix} \overrightarrow{D}_{ij}(k) \\ \Delta t_{V_iV_j}(k) \end{bmatrix} \tag{6}$$

yielding the SD estimates [6],[12]. Next, with an initial estimation of the position of the reference vehicle V_i, Eq.6 can be solved iteratively, resulting in an estimate of $D_{ij}(k)$, which can then be used to determine the distance between both vehicles for each time instant k [12]. Notice that the vehicle distance vector $\overrightarrow{D}_{ij}(k)$, obtained via matrix inversion (Least Square Method) of Eq.6 consists of three distance vector components, i.e., (x, y, z) and one time delay component. For IVD, we used the l_2 norm of the first three components.

2.2.3. Double-Differencing (DD-based) algorithm

In the SD-based algorithm of (6), user clock offsets and common biases among those measurements are still present. To eliminate these uncertainties and also any other common biases, we can utilize a new GNSS measurement and then compute the difference between the SD estimates obtained from two distinct satellites, say S_A and S_B. This is referred to as the double-differencing (DD) algorithm and is demonstrated in Fig.2. The DD-based approach assumes that both vehicles can track satellites S_A and S_B at the same time. Hence, we first apply an SD-based algorithm to each vehicle toward the satellites S_A and S_B, denoted by $\Delta\rho_{V_iV_j}^{S_A}(k)$ and $\Delta\rho_{V_iV_j}^{S_B}(k)$, respectively, which are obtained from (4). Then, each double difference of such quantities defined by $\nabla\Delta\rho_{V_iV_j}^{S_AS_B}(k)$ is obtained as [11]:

$$\nabla\Delta\rho_{V_iV_j}^{S_AS_B}(k) = \Delta\rho_{V_iV_j}^{S_A}(k) - \Delta\rho_{V_iV_j}^{S_B}(k) = \Delta R_{V_iV_j}^{S_AS_B}(k) + \Delta\varepsilon_{V_iV_j}^{S_AS_B}(k) \tag{7}$$

where $\Delta R_{V_iV_j}^{S_AS_B}(k) = \Delta R_{V_iV_j}^{S_A}(k) - \Delta R_{V_iV_j}^{S_B}(k)$ and $\Delta\varepsilon_{V_iV_j}^{S_AS_B}(k) = \Delta\varepsilon_{V_iV_j}^{S_A}(k) - \Delta\varepsilon_{V_iV_j}^{S_B}(k)$. We can then estimate $\Delta R_{V_iV_j}^{S_AS_B}(k)$ using the same trigonometric idea of SD, that is illustrated in Fig.3 [6],[11],[12].

$$\Delta R_{V_iV_j}^{S_AS_B}(k) = [\overrightarrow{u}^{S_A} - \overrightarrow{u}^{S_B}]\overrightarrow{D}_{ij}(k) \tag{8}$$

where $\overrightarrow{u}^{S_A}$ and $\overrightarrow{u}^{S_B}$ are computed as in (5). Using (7) is then possible to calculate the distance and the relative positions of two vehicles. Indeed, using the satellite A as a reference, the solution to the DD-based algorithm according to Fig.3 is given by the matrix form [6],[11]:

$$\begin{bmatrix} \nabla\Delta\rho_{V_iV_j}^{S_1S_A}(k) \\ \nabla\Delta\rho_{V_iV_j}^{S_2S_A}(k) \\ \vdots \\ \nabla\Delta\rho_{V_iV_j}^{S_BS_A}(k) \end{bmatrix} \approx \begin{bmatrix} [u^1 - u^A]^T \\ [u^2 - u^A]^T \\ \vdots \\ [u^N - u^A]^T \end{bmatrix} \overrightarrow{D}_{ij}(k) \tag{9}$$

Notice that the IVD vector $\overrightarrow{D}_{ij}(k)$ is projected in the direction of the difference satellite unitary vectors $\overrightarrow{u}^{S_{AB}} = \overrightarrow{u}^{S_A} - \overrightarrow{u}^{S_B}$ for each DD measurement indicated by $\nabla\Delta\rho_{V_iV_j}^{S_{AB}}(k)$. Assuming four satellites, say S_A, S_B, S_C, and S_D, and considering S_A as the reference satellite, the following system of linear equations derived from (8) can be obtained [11]:

$$\begin{bmatrix} \nabla\Delta\rho_{V_iV_j}^{S_{AB}} \\ \nabla\Delta\rho_{V_iV_j}^{S_{AC}} \\ \nabla\Delta\rho_{V_iV_j}^{S_{AD}} \end{bmatrix} = \begin{bmatrix} u_x^{S_{AB}} & u_y^{S_{AB}} & u_z^{S_{AB}} \\ u_x^{S_{AC}} & u_y^{S_{AC}} & u_z^{S_{AC}} \\ u_x^{S_{AD}} & u_y^{S_{AD}} & u_z^{S_{AD}} \end{bmatrix} \begin{bmatrix} D_x \\ D_y \\ D_z \end{bmatrix} = \boldsymbol{G_{uu}}\overrightarrow{D}_{ij}(k) \tag{10}$$

where:

$$\overrightarrow{u}^{S_{qr}} = \frac{\overrightarrow{S_q}(k) - \overrightarrow{P_{V_i}}(k)}{||\overrightarrow{S_q}(k) - \overrightarrow{P_{V_i}}(k)||} - \frac{\overrightarrow{S_r}(k) - \overrightarrow{P_{V_i}}(k)}{||\overrightarrow{S_r}(k) - \overrightarrow{P_{V_i}}(k)||} = \begin{bmatrix} u_x^{S_q} \\ u_y^{S_q} \\ u_z^{S_q} \end{bmatrix} - \begin{bmatrix} u_x^{S_r} \\ u_y^{S_r} \\ u_z^{S_r} \end{bmatrix}$$

where $\overrightarrow{S_q}$ and $\overrightarrow{S_r}$, $q, r \in \{A, B, C, D\}$ are the satellite position vectors and $\overrightarrow{P_{V_i}}$ is position vector of the vehicle V_i, all evaluated at the time-step k. Notice that 4 is the minimum number

of satellites needed to have a solution of the DD-based algorithm, i.e., $\boldsymbol{G_{uu}}$ (known as the *geometry matrix*) should be non-singular. Usually, if more than 4 satellites are available, a more precise and effective Least Squares solution is adopted.

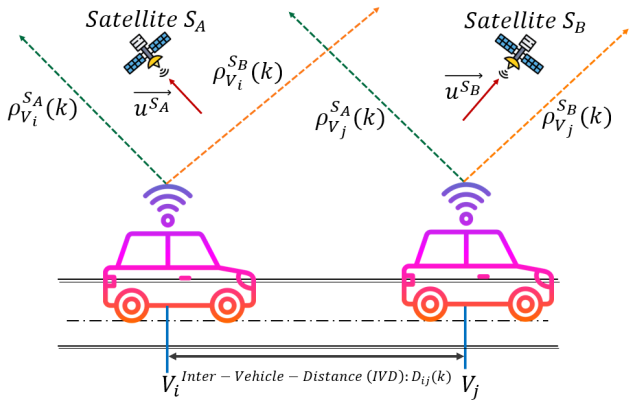

Figure 2: Double-Differencing (DD-based) IVD estimation algorithm

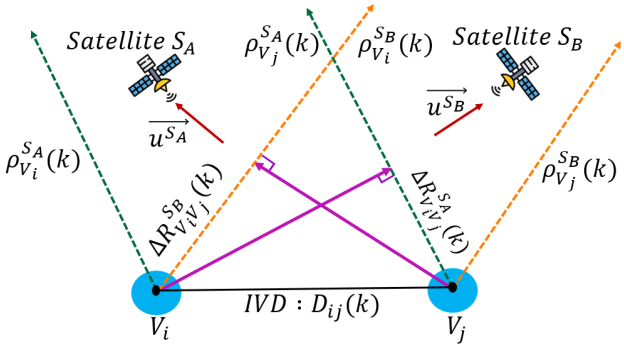

Figure 3: DD-based IVD estimation algorithm and triangle concept

2.3. Geometric dilution of precision (GDOP)

All common GNSS source errors, such as multipath, thermal noise, and atmospheric error, can impact GNSS accuracy and, as a result, estimated IVD. To distinguish among the different satellite configurations, we used the GDOP as a figure of merit for the reachable uncertainty [16–18]. To compute the GDOP, we first assume that all the GNSS range measurements are zero-mean and with equal variance σ_ρ^2, which yields [16–18]:

$$\boldsymbol{W} = \sigma_\rho^2(\boldsymbol{G_{uu}^T G_{uu}})^{-1} = \begin{bmatrix} W_{11} & W_{12} & W_{13} & W_{14} \\ W_{21} & W_{22} & W_{23} & W_{24} \\ W_{31} & W_{32} & W_{33} & W_{34} \\ W_{41} & W_{42} & W_{43} & W_{44} \end{bmatrix} \tag{11}$$

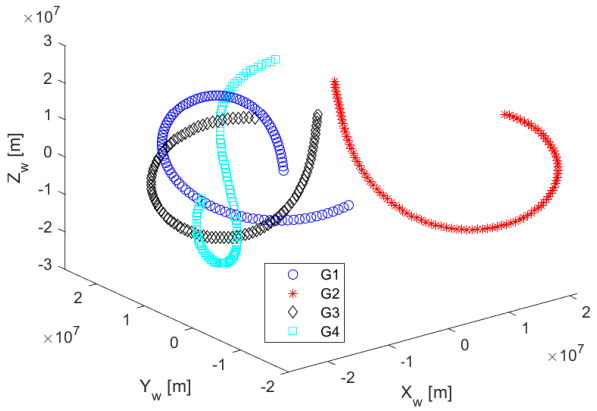

Figure.4 (a): Satellite trajectories

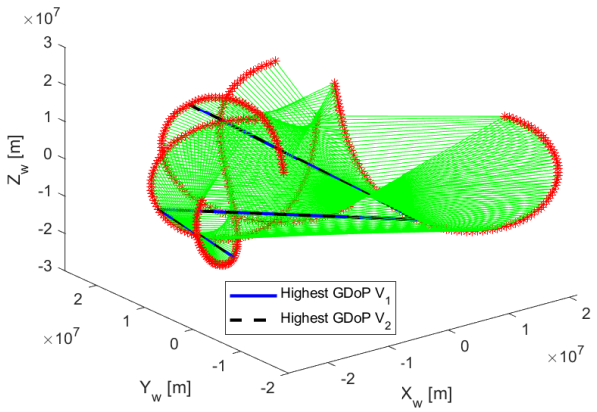

Figure.4 (b): Satellite configuration for each measurement. In Fig.4 (b) satellite paths are depicted in red and GDoP values are shown in green.

Then GDOP is finally given by [16–18]:

$$GDOP = \sqrt{W_{11} + W_{22} + W_{33} + W_{44}}. \tag{12}$$

3. Simulation Configuration

This investigation utilizes Monte-Carlo (MC) simulation in MATLAB® with multiple runs (10,000) with different random errors on the pseudorange measurements. To this end, we

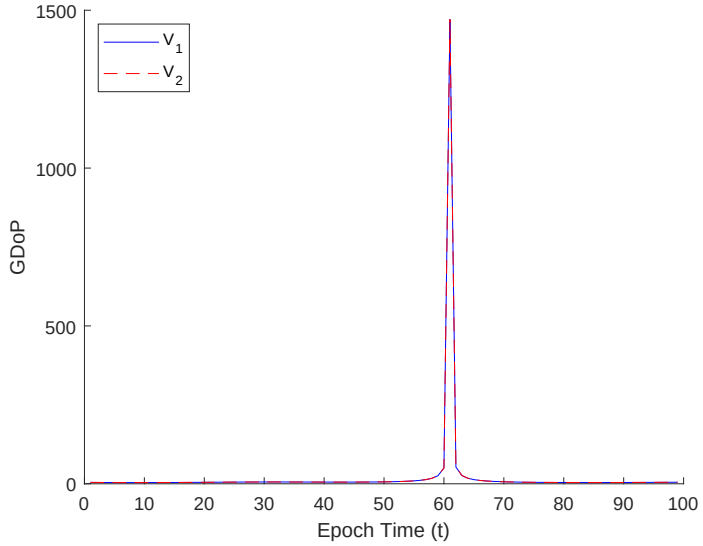

Figure 5: GDOP analysis

assumed four arbitrary constellations of GNSS satellites, i.e., four GPS satellites called $G1$, $G2$, $G3$, and $G4$. As our analysis is a post-processing simulation (i.e., not real-time), we picked 99 satellite locations from International GNSS Service (IGS) data between 00:00 and 08:10 on April 26, 2022 (updated every 5 minutes)[19]. Fig.4 (a) and Fig.4 (b) depict satellite trajectories and configurations for each measurement, with the highest GDOP, highlighted for both vehicles V_1 and V_2, respectively.

Additionally, we considered that two outdoor autonomous vehicles (V_1 and V_2) with LOS views toward GNSS satellites are located at $[4.3495264, 0.8573517, 4.5707671] \times 10^6$ (m) and $[4.3495297, 0.8573477, 4.5707662] \times 10^6$ (m) in the ECEF coordinates, respectively. Hence, after applying the APD given by Eq.3, 5.2 meters is the estimated distance between two vehicles. We assume here that the two autonomous vehicles equipped with the GNSS receivers additionally have a Real-time kinematic (RTK) system that calculates the distance between itself and the broadcasting satellite. Therefore, utilizing the RTK data, the estimated IVD by the APD approach is assumed to be the actual ground truth between the two vehicles [18].

For algorithm simulation, we assumed various levels of pseudorange uncertainty, which were supposed to be uncorrelated and have zero means (i.e., no bias) [6],[12]. Indeed, a random Gaussian error with a standard deviation σ ranging from zero to one by step 0.1 was added to each pseudorange measurement. Furthermore, we compute two statistical metrics, the standard deviation and average absolute error on IVD estimation, concerning the ground truth (5.2m). More precisely, in our study, the average error and standard deviation error define the mean error and the standard deviation of the absolute error on IVD measurements for each algorithm over 10,000 MC trials, respectively. Lastly, notice that in our simulation, $\sigma = 0$ (m) is just for the algorithm's sanity check under ideal conditions [18].

The further point is that when simulating cooperative positioning algorithms with multiple satellite systems, we examined Single Differencing (SD) and Double Differencing (DD) at each

epoch using four satellite pseudoranges. Moreover, in Single Differencing with Single Satellite (SD-SS), at each epoch, all the pseudoranges from the same satellite are utilized, i.e., at the k-th epoch, all the pseudoranges from 1 to k are used. Hence, data are available for $k > 3$ [6],[12].

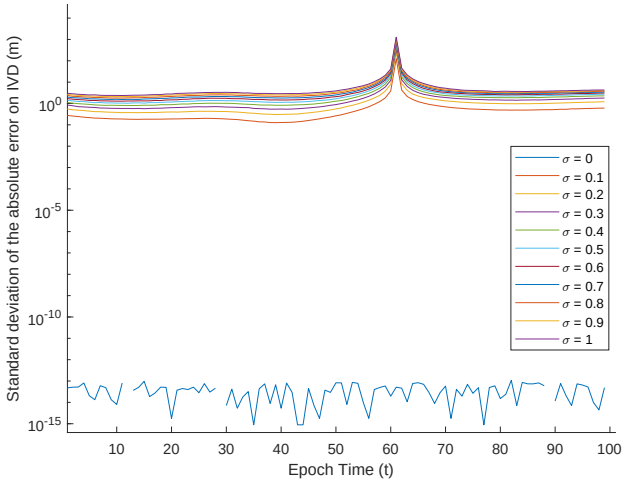

Figure.6 (a): The standard deviation of the absolute error on IVD in SD-based algorithm

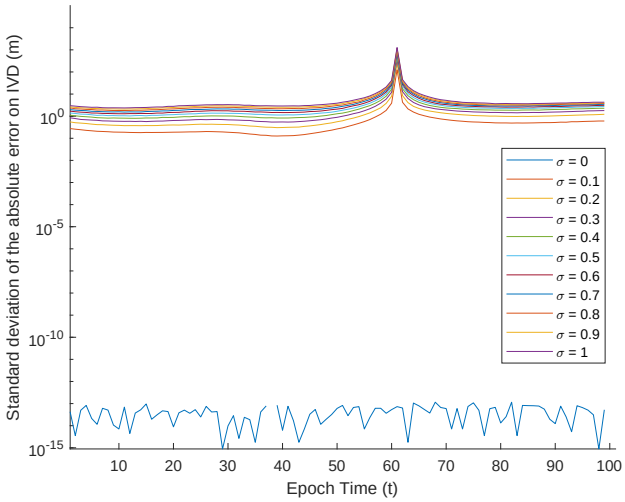

Figure.6 (b): The standard deviation of the absolute error on IVD in DD-based algorithm

4. Results and Discussion

Fig.5 depicts the GDoP analysis during 99 epochs for two vehicles, V_1 and V_2. From Fig.5, we noticed a large error around the epoch 61^{st} and assume it was a GDoP issue. Indeed, if we take

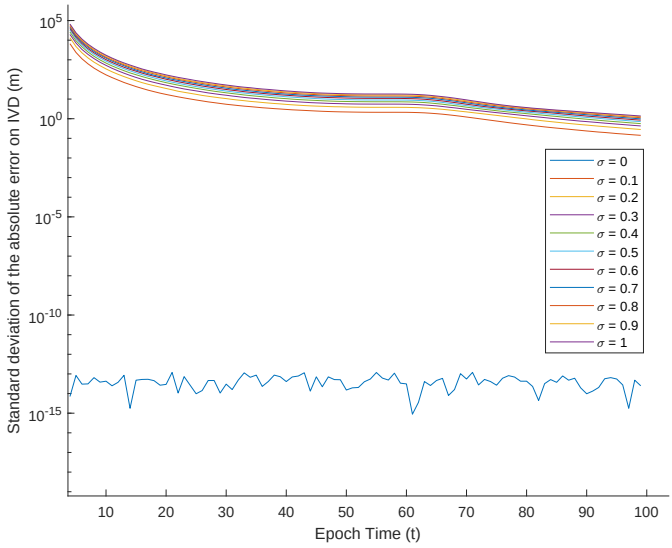

Figure.6 (c): The standard deviation of the absolute error on IVD in SD-SS algorithm

a look at the satellite paths (see Fig.4 (a) for reference), there may be moments in which the four satellites are aligned on a plane. This is evident from the satellite configuration, in which a line connects the satellite used for each epoch time. We may see the thick line of the configuration returning the highest GDoP (Fig.5). This is a purely (and known) geometric problem with (pseudo) ranging systems, so it is all aligned with the theory (as it should be)[16–18].

As mentioned in the literature review, the non-ranging cooperative localization algorithms employing multiple satellites, such as SD and DD, may provide higher accuracy in IVD estimates. This statement is validated in this study through simulation. To this end, consider Fig.6 (a), (b), and (c), which illustrates the standard deviation of the absolute error on IVD estimation for SD, DD, and SD-SS algorithms, respectively. The most interesting aspect of comparing Fig.6 (a) and Fig.6 (b) is that there is no significant difference between SD- and DD-based techniques when the number of employed satellites is four. In contrast, by comparing Fig.6 (a) and Fig.6 (b) with Fig.6 (c), it can be evidently seen that the standard deviation of the absolute error on IVD estimation in either SD or DD algorithms is roughly 10^0(m), which is much smaller than the SD-SS algorithm, which is between $\approx [10^0, 10^5]$(m), demonstrating the role of using multiple satellites to achieve lower uncertainty for IVD estimation.

Furthermore, Fig.7 (a), (b), and (c) show the average absolute error on IVD estimates for the SD, DD, and SD-SS approaches, respectively. In the same way, the SD and DD-based methods functioned identically in terms of an average absolute error on IVD estimation. However, when comparing Fig.7 (a) and (b) with Fig.7 (c), the DD (SD)-based algorithm has a lower average absolute error on IVD estimation $\approx [10^{-2}, 10^0]$(m) than the SD-SS algorithm $\approx [10^{-4}, 10^4]$(m), thus further verifying the message of this paper: using multiple satellite systems (multi-GNSS) benefits the uncertainty related to the inter-vehicle distance. This is also asserted in [13],[14], which refers to the use of multi-GNSS systems to achieve better (centimeter-level) accuracy in satellite-based positioning approaches. Finally, notice that when employing the DD-based

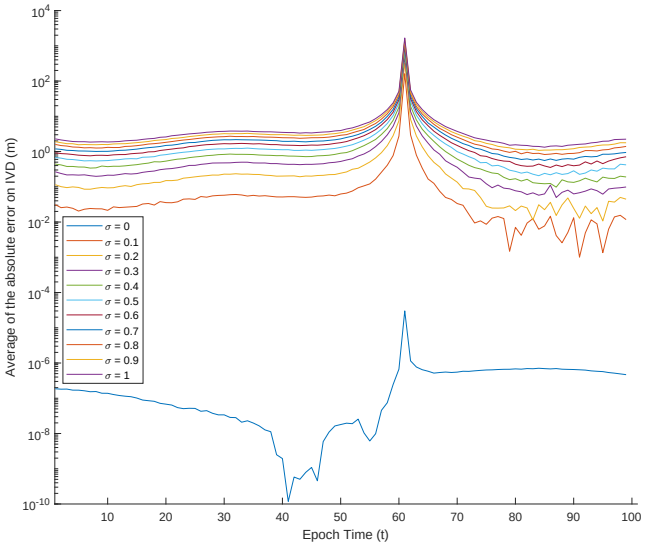

Figure.7 (a): The average of the absolute error on IVD in SD-based algorithm

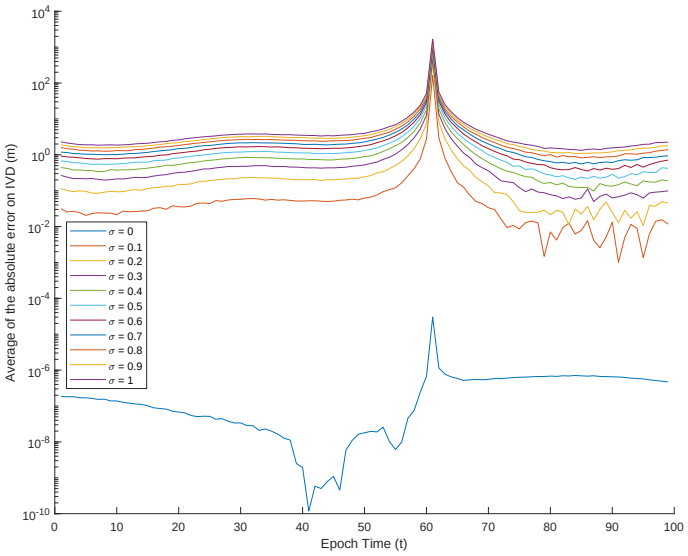

Figure.7 (b): The average of the absolute error on IVD in DD-based algorithm

technique, biases from multiple GNSS satellites can be eliminated, which is a considerable advantage for DD-based algorithm.

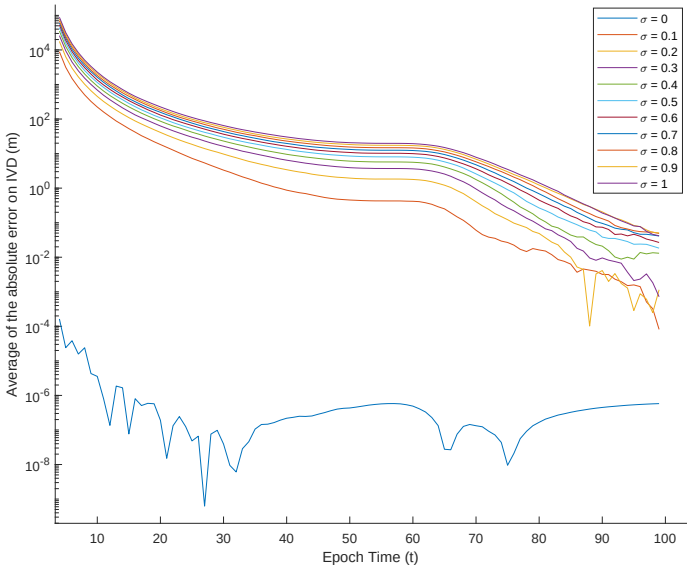

Figure.7 (c): The average of the absolute error on IVD in SD-SS algorithm

5. Conclusion

In this study, we used Monte-Carlo simulations to assess the performance of four non-ranging-based cooperative positioning algorithms such as APD, SD, SD-SS, and DD for the IVD estimation problem. The simulation results demonstrated that when four satellites were employed for IVD estimation, there was no considerable difference between SD- and DD-based algorithms. Indeed, it appears that the systematic effects influencing the pseudorange measurements have been cancelled out. Hence, it can be concluded that more accurate IVD estimation will be achieved if more than four satellites are available. Furthermore, this investigation showed that the DD-based technique has a lower average IVD error $\approx [10^{-2}, 10^{0}]$(m), than the SD-SS approach $\approx [10^{-4}, 10^{4}]$(m), suggesting that a DD-based algorithm with multiple satellite systems can be employed to achieve higher accuracy in IVD estimation problem.

Further research can be defined to determine the effectiveness of the proposed cooperative localization algorithms, while the vehicles are moving at different speeds and different directions. Moreover, investigation and experimentation into IVD estimation accuracy using a reliable method of merging additional data, such as the use of multiple GNSS satellites is recommended. Finally, further experiments employing the real pseudorange measurements with more than four satellites, could provide more insight into more realistic IVD estimation problem.

Acknowledgments

This research was supported by Centro Ricerche Fiat (CRF) and imec–WAVES research group at Ghent University.

References

[1] S. Kuutti, S. Fallah, K. Katsaros, M. Dianati, F. Mccullough, A. Mouzakitis, A Survey of the State-of-the-Art Localization Techniques and Their Potentials for Autonomous Vehicle Applications, in: IEEE Internet of Things Journal, vol. 5, no. 2, pp. 829-846, April 2018, doi: 10.1109/JIOT.2018.2812300.

[2] L. Huang, T. Zhe, J. Wu, Q. Wu, C. Pei, D. Chen, Robust Inter-Vehicle Distance Estimation Method Based on Monocular Vision, in: IEEE Access, vol. 7, pp. 46059-46070, 2019, doi: 10.1109/ACCESS.2019.2907984.

[3] R. C. Daniels, E. R. Yeh, R. W. Heath, Forward Collision Vehicular Radar With IEEE 802.11: Feasibility Demonstration Through Measurements, in: IEEE Transactions on Vehicular Technology, vol. 67, no. 2, pp. 1404-1416, Feb. 2018, doi: 10.1109/TVT.2017.2758581.

[4] M. Miljković, M. Vranješ, D. Mijić, M. "ukić, Vehicle Distance Estimation Based on Stereo Camera System with Implementation on a Real ADAS Board, in: Proceedings of the 2022 International Conference on Software, Telecommunications and Computer Networks (SoftCOM), 2022, pp. 1-6, doi: 10.23919/SoftCOM55329.2022.9911360.

[5] J. Fayyad, M. A. Jaradat, D. Gruyer, H. Najjaran, Deep Learning Sensor Fusion for Autonomous Vehicles Perception and Localization: A Review, in: Sensors-special issue "Sensor Data Fusion for Autonomous and Connected Driving", 2020, 20 (15), 35p. ff10.3390/s20154220ff.ffhal-02942600f

[6] F. Wang , W. Zhuang , G. Yin, S. Liu, Y. Liu, H. Dong, Robust Inter-Vehicle Distance Measurement Using Cooperative Vehicle Localization, in: Sensors 2021, 21(6), 2048; https://doi.org/10.3390/s21062048.

[7] N. Saeed, W. Ahmad, D. M. S. Bhatti, Localization of vehicular ad-hoc networks with RSS based distance estimation, in: Proceedings of the 2018 International Conference on Computing, Mathematics and Engineering Technologies (iCoMET), 2018, pp. 1-6, doi: 10.1109/ICOMET.2018.8346313.

[8] J. Yin, Q. Wan, S. Yang, K. C. Ho, A Simple and Accurate TDOA-AOA Localization Method Using Two Stations, in: IEEE Signal Processing Letters, vol. 23, no. 1, pp. 144-148, Jan. 2016, doi: 10.1109/LSP.2015.2505138.

[9] H. Cao, Y. Wang, J. Bi, S. Xu, M. Si, H. Qi, Indoor positioning method using WiFi RTT based on LOS identification and range calibration, in: ISPRS International Journal. Geo-Inf., vol. 9, no. 11, p. 627, Oct. 2020

[10] J. He, H. C. So, A Hybrid TDOA-Fingerprinting-Based Localization System for LTE Network, in: IEEE Sensors Journal, vol. 20, no. 22, pp. 13653-13665, 15 Nov.15, 2020, doi: 10.1109/JSEN.2020.3004179.

[11] F. de Ponte Müller, E. M. Diaz, B. Kloiber, T. Strang, Bayesian cooperative relative vehicle positioning using pseudorange differences, in: Proceedings of the 2014 IEEE/ION Position, Location and Navigation Symposium-PLANS 2014, 2014, pp. 434-444, doi: 10.1109/PLANS.2014.6851401.

[12] M. Tahir, S. S. Afzal, M. S. Chughtai, K. Ali, On the Accuracy of Inter-Vehicular Range Measurements Using GNSS Observables in a Cooperative Framework, in: IEEE Transactions on Intelligent Transportation Systems, vol. 20, no. 2, pp. 682-691, Feb. 2019, doi: 10.1109/TITS.2018.2833438.

[13] M. Alijani, A. Steccanella, D. Fontanelli, Cooperative Positioning Algorithms for Estimating Inter-Vehicle Distance Using Multi-GNSS, in: Proceedings of the 2023 IEEE International Instrumentation and Measurement Technology Conference (I2MTC), Kuala Lumpur, Malaysia, 2023, pp. 1-6, doi: 10.1109/I2MTC53148.2023.10176082.

[14] T. Kong, L. Ma, G. Ai, Research on Improving Satellite Positioning Precision Based on Multi-Frequency Navigation Signals, in: Sensors 2022, 22(11), 4210; https://doi.org/10.3390/s22114210.

[15] M. Khider, T. Jost, E. Abdo Sánchez, P. Robertson, M. Angermann, Bayesian multisensor navigation incorporating pseudoranges and multipath model, in: Proceedings of the IEEE/ION Position, Location and Navigation Symposium, Indian Wells, CA, 2010, pp. 816-825, doi: 10.1109/PLANS.2010.5507321.

[16] F. Shamsfakhr, A. Antonucci, L. Palopoli, D. Macii, D. Fontanelli, Indoor Localization Uncertainty Control Based on Wireless Ranging for Robots Path Planning, in: IEEE Trans. on Instrumentation and Measurement, vol. 71, pp. 1-11, 2022.

[17] I. Sharp, K. Yu, Y. J. Guo, GDOP Analysis for Positioning System Design, in: IEEE Transactions on Vehicular Technology, vol. 58, no. 7, pp. 3371-3382, Sept. 2009, doi: 10.1109/TVT.2009.2017270.

[18] P. Misra, P. Enge, Global Positioning System: Signals, Measurement and Performance (Revised 2nd Edition), Revised 2nd Edition Published in 2011, Ganga-Jamuna Press, P.O. Box 633, Lincoln, MA 01773.

[19] URL: https://cddis.nasa.gov/archive/gnss/data/hourly/, (Last accessed April. 26, 2022).